NIST Technical Note XXXX

Measurement of the Flow Resistance of Vegetation

Ryan Falkenstein-Smith
Kevin McGrattan
Marco Fernandez

This publication is available free of charge from:
https://doi.org/10.6028/NIST.TN.XXXX

National Institute of
Standards and Technology
U.S. Department of Commerce

NIST Technical Note XXXX

Measurement of the Flow Resistance of Vegetation

Ryan Falkenstein-Smith
Kevin McGrattan
Marco Fernandez
Fire Research Division
Engineering Laboratory

This publication is available free of charge from:
https://doi.org/10.6028/NIST.TN.XXXX

Month Year

U.S. Department of Commerce
Wilbur L. Ross, Jr., Secretary

National Institute of Standards and Technology
Walter Copan, NIST Director and Undersecretary of Commerce for Standards and Technology

National Institute of Standards and Technology Technical Note XXXX
Natl. Inst. Stand. Technol. Tech. Note XXXX, 19 pages (Month Year)
CODEN: NTNOEF

This publication is available free of charge from:
https://doi.org/10.6028/NIST.TN.XXXX

Abstract

This report documents the measurement of the wind resistance of different types of vegetation. The measurements are made in a wind tunnel with a 2 m test section and 0.5 m by 0.5 m cross-section. Samples of vegetation have been cut into cubical volumes that span the cross-section of the tunnel. The wind resistance is inferred via measurement of the pressure drop across the sample at wind speeds ranging from 2 m/s to 8 m/s. The results are compared to empirical correlations quantifying the wind resistance of regularly spaced vertical tubes of comparable geometric characteristics.

Key words

Vegetation Canopy; Drag Coefficient; Wind Tunnel

Table of Contents

List of Tables

List of Figures

1. Introduction

The Fire Research Division of the National Institute of Standards and Technology (NIST) has developed several numerical models to predict the behavior of fires within buildings. One of the models, a computational fluid dynamics (CFD) code called the Fire Dynamics Simulator (FDS) [1], has been extended to model fires in the wildland-urban interface (WUI). One crucial component of this type of modeling is a proper treatment of wind-driven flow through vegetation. The objective of the experiments described in this report is to measure the drag coefficient of an empirical sub-model appropriate for CFD.

Measurements of this type have been performed by other researchers [2–6], most of whom used wind tunnels of various sizes. In most cases, a single plant or small tree was positioned within the tunnel and the resistance force measured. However, such a measurement is not readily applicable to a CFD model which does not necessarily consider the tree as a whole but rather as a volume occupied by subgrid-scale objects that decrease momentum in the grid cells that they occupy. Some plants might be smaller than a characteristic grid cell, and some trees might be larger, but in either case, these objects are just momentum sinks within individual grid cells that require some drag coefficient that is appropriate to the local conditions. That is, it is not appropriate to talk about the "freestream velocity" within a CFD model, as the velocity changes from cell to cell.

2. Model Development

Consider a volume filled with a random collection of leaves, pine needles, or other types of vegetation, as shown in Fig. 1. This volume can be regarded as a single grid cell in a CFD model for which the computational domain may span hundreds to thousands of meters. At a given instant in the numerical simulation, this grid cell would have, at the very least, an average flow speed, U, and gas density, ρ. The vegetation within the cell is typically modeled as a collection of subgrid-scale Lagrangian particles whose mass, size, and shape are characterized by a handful of parameters that can be determined with field measurements. These particles exert a force per unit volume given by:

$$F = \frac{1}{V}\frac{\rho}{2}\sum_{i=1}^{N} C_{\mathrm{d}} A_{\mathrm{p},i} U^2 \tag{1}$$

where V is the volume of the grid cell, $A_{\mathrm{p},i}$ is the projected area of the ith vegetative component, and C_{d} is a drag coefficient which is taken as a constant. Similar configurations have already been been adapted in numerical investigations [7, 8].

Equation (1) can be recast in an equivalent form that is more useful for describing vegetation drag [9]:

$$F = \frac{\rho}{2} C_{\mathrm{d}} C_{\mathrm{s}} \beta \sigma U^2 \tag{2}$$

where C_{s} is a shape factor defined in this case as the average ratio of the projected area to surface area of the vegetative elements, β is the ratio of the volume occupied by vegetation

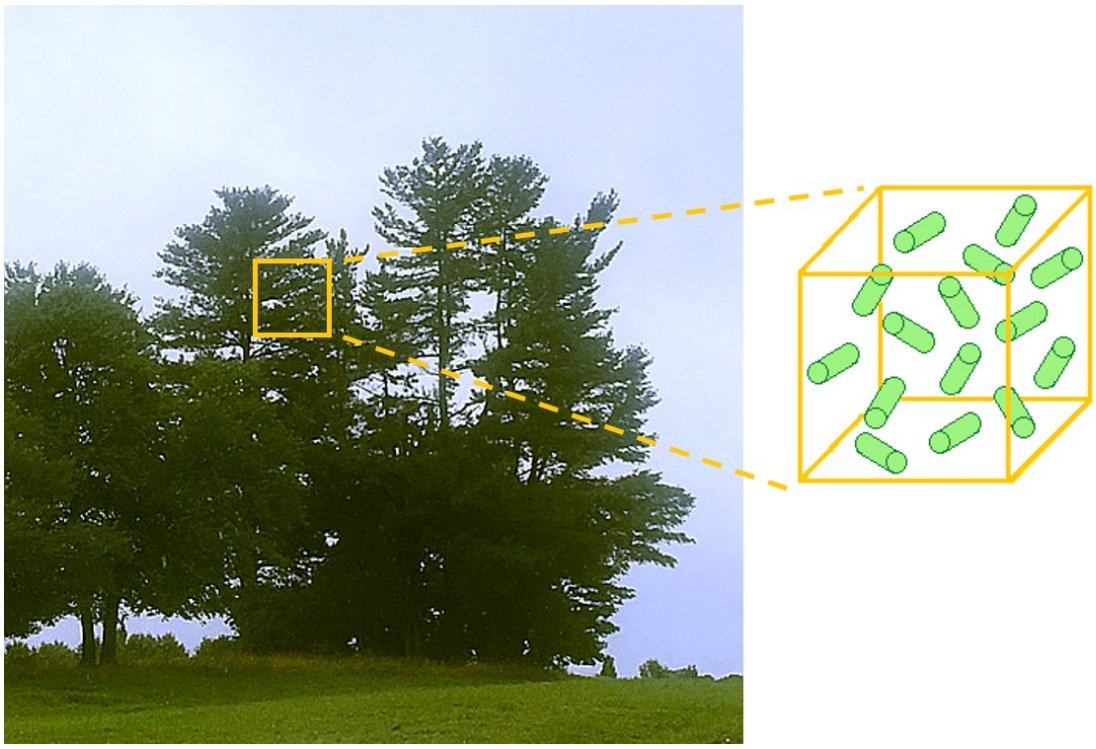

Fig. 1. Vegetation translation to multi-component model

to the volume of the grid cell, V, and σ is an average surface area to volume ratio of the vegetative elements. Some of the terms are difficult to measure, such as the shape factor and surface to volume ratio. However, these terms may be combined to form a parameter that resembles an absorption coefficient:

$$\kappa = C_{\mathrm{s}}\,\beta\,\sigma \tag{3}$$

that can be determined by measuring the projected area of light passing a distance L through the vegetation. The relative area of light, or "free-area coefficient", is defined by the relation:

$$W = \mathrm{e}^{-\kappa L} \tag{4}$$

In the experiments, the cross-section of a small wind tunnel is filled with various amounts and types of vegetation to determine the drag coefficient for the following simplified model:

$$F \equiv \frac{\Delta P}{L} = \frac{\rho}{2} C_{\mathrm{d}}\,\kappa U^2 \tag{5}$$

3. Description of Experiments

3.1 Sample Preparation

The vegetation chosen for this work was a Bakers Blue Spruce (*Picea pungens 'Bakeri'*), an Evergreen Distylium (Distylium 'PIIDIST-I' Plant Patent #24410), a Gold Rider Leyland Cypress (*Cupressocyparis leylandii 'Gold Rider'*), a Kimberly Queen Fern (*Nephrolepis obliterata 'Kimberly Queen'*), a Blue Shag Eastern White Pine (*Pinus strobus 'Blue Shag'*), and a Robin Red Holly (*Ilex opaca*). Each sample was chosen based on its local availability. Leaf shapes were varied, including needle, elliptic, scale, and ovate.

The plant samples were cut into 0.5 m by 0.5 m by 0.5 m cubes using a guiding frame (Fig. 2). The samples completely filled the cross section of the wind tunnel forcing the flow to move through the vegetation as opposed to around it. To easily distinguish the front, back, left, and right side of the cube-shaped vegetation, each side was designated position A (PA), position B (PB), position C (PC), or position D (PD) (Fig. 3). After its initial cut, image analysis, wind tunnel measurements, and water displacement testing were conducted in subsequent order. In some cases, additional cuts were made to certain samples at the conclusion of the experimental procedure. The decision to make additional cuts made to the vegetation samples mainly depended on the health of the plant after an iteration in the experimental procedure. In the case of the Bakers Blue Spruce, Gold Rider Leyland Cypress, and Robin Red Holly, four iterative cuts were made with the final cut being the removal of all leaves from the vegetation.

3.2 Determining the Free-Area Coefficient via Photography

The absorption coefficient of the vegetation samples were determined from the free-area coefficient (W) of the projected area of the sample. To determine this, the sample was placed on a table located between a large white backdrop and a 0.5 m by 0.5 m cardboard frame (Fig. 4), the same dimensions as the wind tunnel, providing an accurate representation of the vegetation's projected area when placed within the tunnel. For each sample cut and position, the projected area was photographed. All images were captured using a Nikon D5600 camera placed on a tripod located approximately 3.6 m away from the frontal plane of the vegetation sample. In order to identify smaller areas of white space, the white backdrop was illuminated using a collection of incandescent and LED lights.

The images were processed using MATLAB's Image Processing Toolbox. Imported colored images were first converted into a grey scale and then a binary (black and white) image using a pre-set threshold level. The binary images were then cropped within the cardboard frame to eliminate non-vegetative substances and to evaluate the projected image of the vegetation exclusively. Once the projected image was obtained, a pixel count was conducted to determine the free-area coefficient of the vegetation.

The uncertainty of the free-area coefficients was determined by measuring the projected areas of objects with pre-determined sizes through the same evaluation process. A bias uncertainty of 1 % from the true free-area coefficient was defined for all investigated objects

Fig. 2. Cutting procedure of vegetation samples

Fig. 3. Prepared vegetation sample's designated orientation

with pre-determined sizes. The bias uncertainty was assumed for all free-area coefficients of the vegetation sample configurations.

3.3 Description of the Wind Tunnel

Pressure loss measurements were obtained in a wind tunnel test section with a cross-sectional area of 0.5 m by 0.5 m and a length of 2 m. An image and schematic diagram of the wind tunnel setup is shown in Fig. 5. The volume flow through the tunnel was measured upstream of the vegetation using a Rosemont 485 Annubar. The pressure drop across the vegetation was measured using an MKS Baratron Type 220D pressure transducer with a range of 0 to 133 Pa (1 torr). The air flow was provided by a 0.91 m axial fan controlled by a variable frequency drive and monitored using the Annubar. Air density was calculated from the tunnel's internal temperature measured with a Type-K thermocouple. Each sample configuration was subjected to nine different fan speeds ranging from 0 to 88 % of the full-scale fan speed. The fan speed was not run at full scale due to the risk of exceeding the pressure transducer's pressure limitations. Data was sampled at 90 Hz for a 30 s period while maintaining a constant fan speed.

Once a set of measurements were taken at all fan speeds, the wind tunnel was shut off for approximately 5 min, and then the measurements were repeated. All measurements were repeated three times for each vegetation configuration. The variance homogeneity of the replicate measurements was tested using Hartley's F_{max} test. If it was found that the data sets were homogenous, then the measurements were averaged.

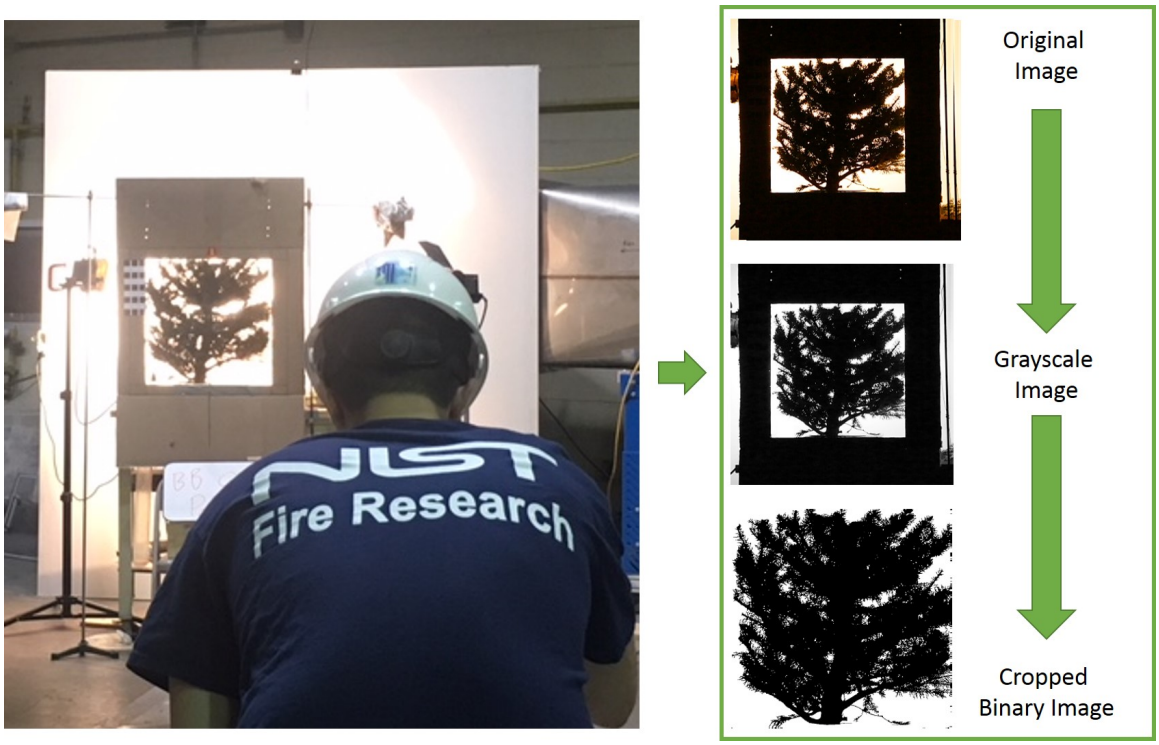

Fig. 4. Setup for photographing vegetation samples (left) and the post-processing procedure for analyzing images (right)

The uncertainty of the pressure readings was determined by combining the precision uncertainty of the acquired data and the bias uncertainty of the pressure transducer. The air density was calculated from the precision error of the acquired data. Velocity uncertainty was established through the propagation of uncertainty that combined pressure and air density uncertainties. The drag coefficient uncertainty was also determined from the propagation of uncertainty, accounting for the pressure, air density and velocity uncertainties in addition to the absorption coefficient bias uncertainty.

3.4 Determining the Volume of Vegetation via Water Displacement

The volume of vegetation was measured following a cut to the vegetation sample. The vegetation was separated into two groups of branches and leaves which were packaged using a cloth mesh bag and thin wire. The volume and mass of the mesh bag and wire were pre-determined and subtracted from the total measured volume to determine the volume the vegetative solid. Before submerging the packaged material, the dry weight of the sample was measured using a Mettler Toledo Jaguar load cell. Before submerging the packaged vegetative solid, the water level was constrained to the bottom lip of a spout located approximately 3.8 cm from the top of the bucket. When the packaged vegetation was submerged, the displaced water was fed through the spout and into a glass beaker (Fig. 6). After the wa-

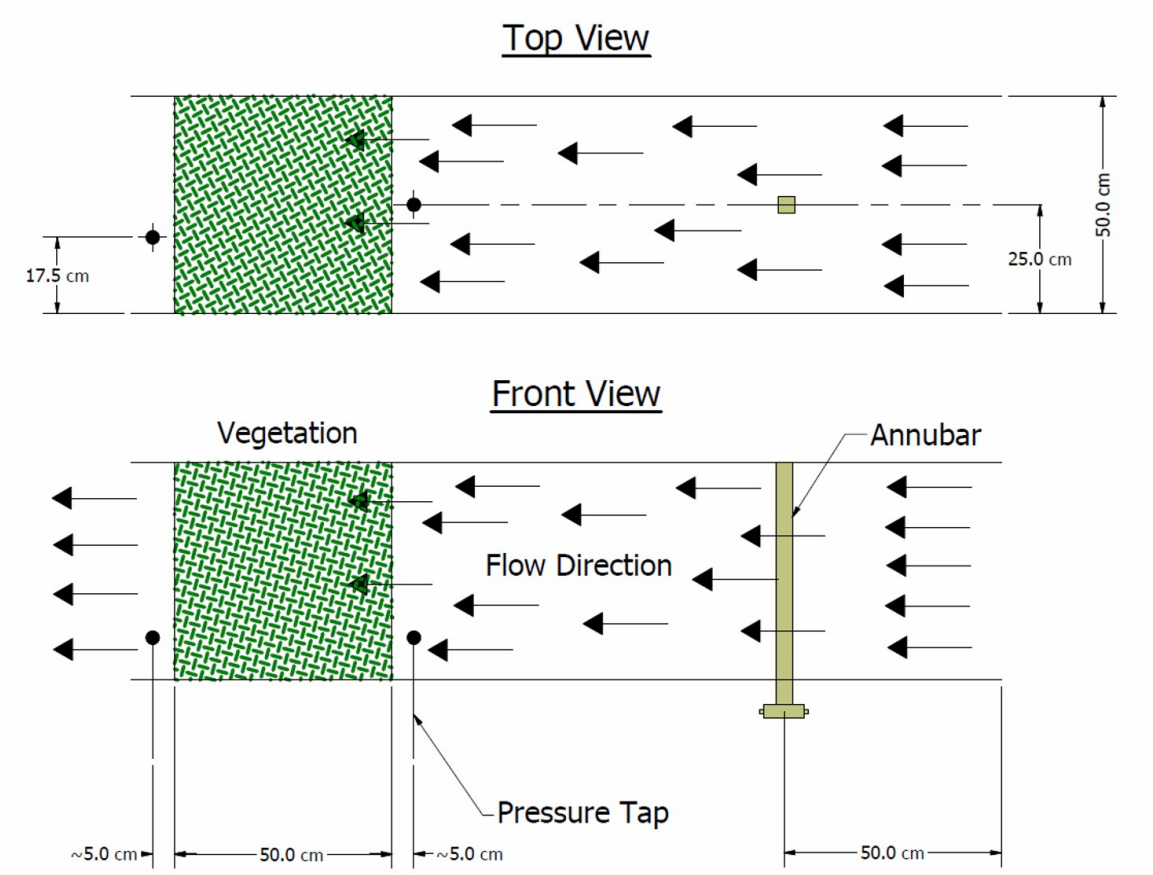

Fig. 5. Wind tunnel experimental setup with top and front schematic drawings

ter flow through the spout of the bucket subsided, the volume of displaced water measured in a 1000 ml graduated cylinder to determine the volume of vegetation. The measurement was repeated three times for each vegetation configuration. The weight of the vegetation was measured in between the displacement tests to account for any additional water that remained after the previous test. The volume ratio, β, was calculated by dividing the average vegetation volume by the volume it occupied (0.5 m $\times$ 0.5 m $\times$ 0.5 m = 0.125 m^3). The uncertainty of the vegetation volume and its respective solid fraction was established by combining the precision uncertainty of the repeated volume measurements and the bias error of the Mettler Toledo load cell (0.005 kg).

Fig. 6. Procedure of the water displacement test

4. Results

The key results of this work are the relationship between the absorption coefficient and solid fraction and more importantly the drag coefficient derived from the measurements made in the Image Analysis and Wind Tunnel Experiments.

4.1 Relationship between the absorption coefficient κ and solid fraction β

Figure 7 presents the relationship between the absorption coefficient and solid fraction of all sample configurations. The markers indicate the measured values while the dotted lines represent a linear regression fit. The linear regression fittings suggest that the absorption coefficient declines with a decrease in the solid fraction. The reduction in the solid fraction corresponds to a cut made on the vegetation sample indicating that the removal of solid material from the vegetation sample modifies the projected free-area coefficient of the canopy, thus decreasing the absorption coefficient. The strong relationship between the absorption coefficient and the solid fraction demonstrated by high the coefficients of determination (r^2) support the formation of the absorption coefficient parameter (Eq. 3).

One unique component of Fig. 7 is the linear regression fitting of the Robin Red Holly. As the solid fraction decreases, the absorption coefficient should approach zero, as demonstrated by most samples. The Robin Red Holly, however, is offset; exhibiting similar absorption coefficient values relative to the other examples despite having a higher solid fraction. The reason for this discrepancy is due to the ratio between branch and leaf and their contributions to the solid fraction and surface to volume ratio. As shown in Table 1, the volume ratio between branches and leaves of the Robin Red Holly is substantially higher relative to the other samples and does not significantly differ between cut iterations. As a result, the surface to volume ratio decreases from the removal of leaves, thus reducing the absorption coefficient, while still maintaining a relatively consistent solid fraction due to the significant volume contribution of the branches.

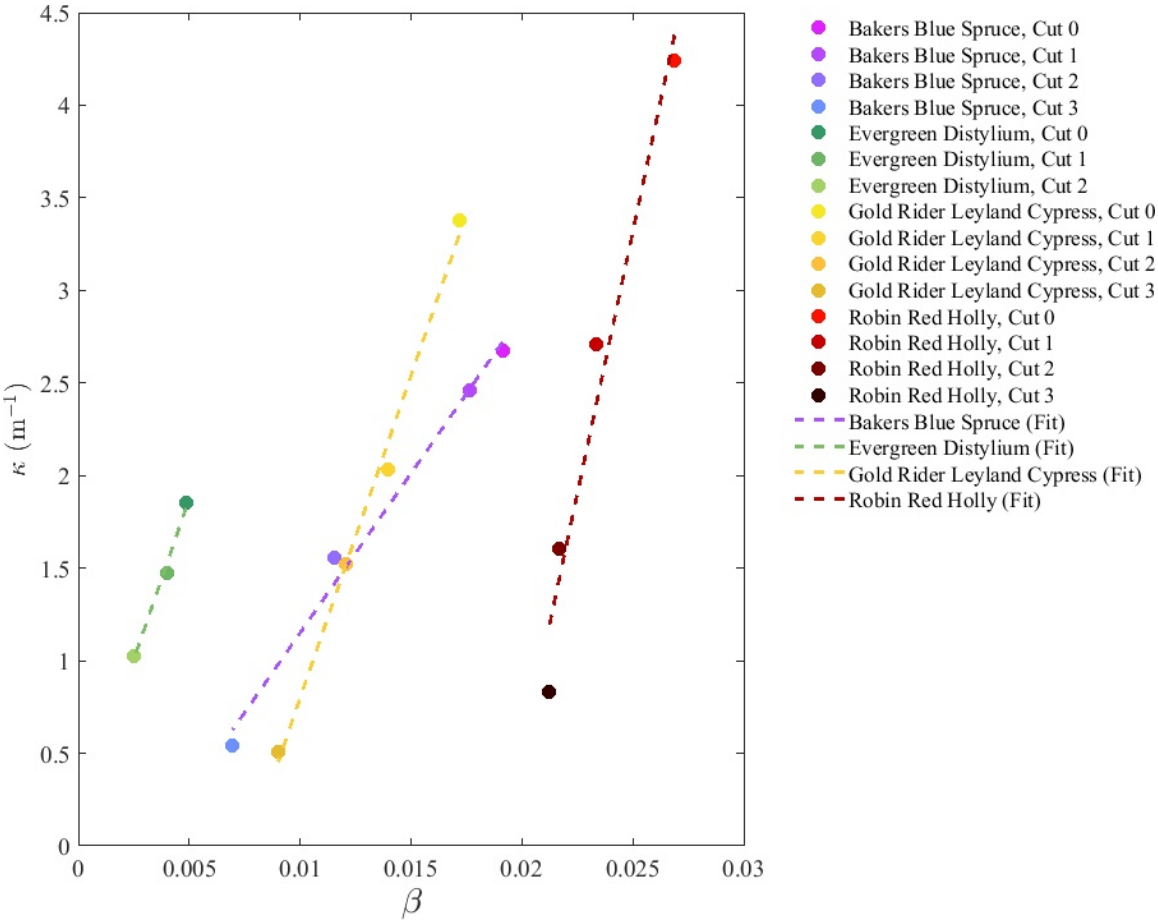

Fig. 7. Calculated absorption coefficients (κ) of vegetation sample configuration plotted against their corresponding solid fractions (β)

Table 1. Branch and leaf volume ratio of vegetation samples with mulitple cut iterations

Sample	Cut	$\frac{\text{Branch Volume}}{\text{Leaf Volume}}$	Sample	Cut	$\frac{\text{Branch Volume}}{\text{Leaf Volume}}$
Bakers Blue Spruce	0	1.1	Gold Rider Leyland Cypress	0	1.5
	1	1.3		1	2.2
	2	1.5		2	3.0
	3	N/A		3	N/A
Evergreen Distylium	0	1.0	Robin Red Holly	0	11
	1	1.4		1	16
	2	3.3		2	47
				3	N/A

4.2 Vegetation Canopy Drag Coefficients

Figure 8 displays the relationship between the freestream velocity and the pressure drop for each sample configuration. The results demonstrate the expected quadratic relationship. Replotting the data as shown in Fig. 9 yields the drag coefficient for each sample configuration as determined by calculating the slope of each line of data points. No linear regression fitting was observed to have a coefficient of determination value less than 0.98, indicating a close representation of the fitted regression line to the measured data. A summary of all 68 calculated drag coefficients and their respective uncertainties are presented in Table 2.

The distribution of all sample configurations' drag coefficient is shown in Fig. 10. A Kolmogorov-Smirnov test (K-S test) was implemented to test the normality of the drag coefficient data. The K-S test determined that the drag coefficients of all sample configurations do not significantly vary from normality, D(68)= 0.09, non-significant. The normal distribution of the data is further supported by the "bell curve" fitting displayed in Fig. 10. Additionally, the average drag coefficient of all sample configurations was determined to be 2.8 with a standard deviation of 0.6.

A one-way analysis of variance (ANOVA) was implemented on the drag coefficients of the different vegetation species. The analysis of the different vegetation species yielded a significant variation among the species, $F(5,62)= 4.88$, $p= 7.97\text{E-}4$. A Tukey HSD test subsequently applied to identify which species' average drag coefficients were significantly different from each other. The results showed one significant difference between the species' average drag coefficients: the Robin Red Holly and Gold-Rider Leyland Cypress. Despite this statistically significant difference, the average drag coefficients of the Robin Red Holly and Gold-Rider Leyland Cypress are both within one standard deviation away from the overall average drag coefficient, as demonstrated in Fig. 10, and therefore is not large enough to have a practical implication. It can then be concluded that the variance of drag coefficients determined for each species is non-significant meaning the overall average drag coefficient presented in Fig. 10 could be applied as a consistent drag coefficient for vegetation canopies in CFD models.

5. Comparison Between Vegetation Data and Tube Bank Models

In comparison to previous work [2–6], the magnitude of the measured drag coefficients in this study is relatively large. As discussed in Section 1, most previous studies have measured the wind resistance of a single plant or tree within a larger wind tunnel while this work considered a relatively homogenous distribution of vegetation within a tunnel. The interpretation of "freestream" velocity, shape factor, cross-sectional area, and so on, are often different in these studies, making it difficult to compare drag coefficients from one study to another. Within the field, there is no single definition of drag coefficient in regard to vegetation.

As a way to verify the accuracy of our wind tunnel measurements and the validity of our drag coefficient derivation, we considered a bank of regularly-spaced, staggered, vertical

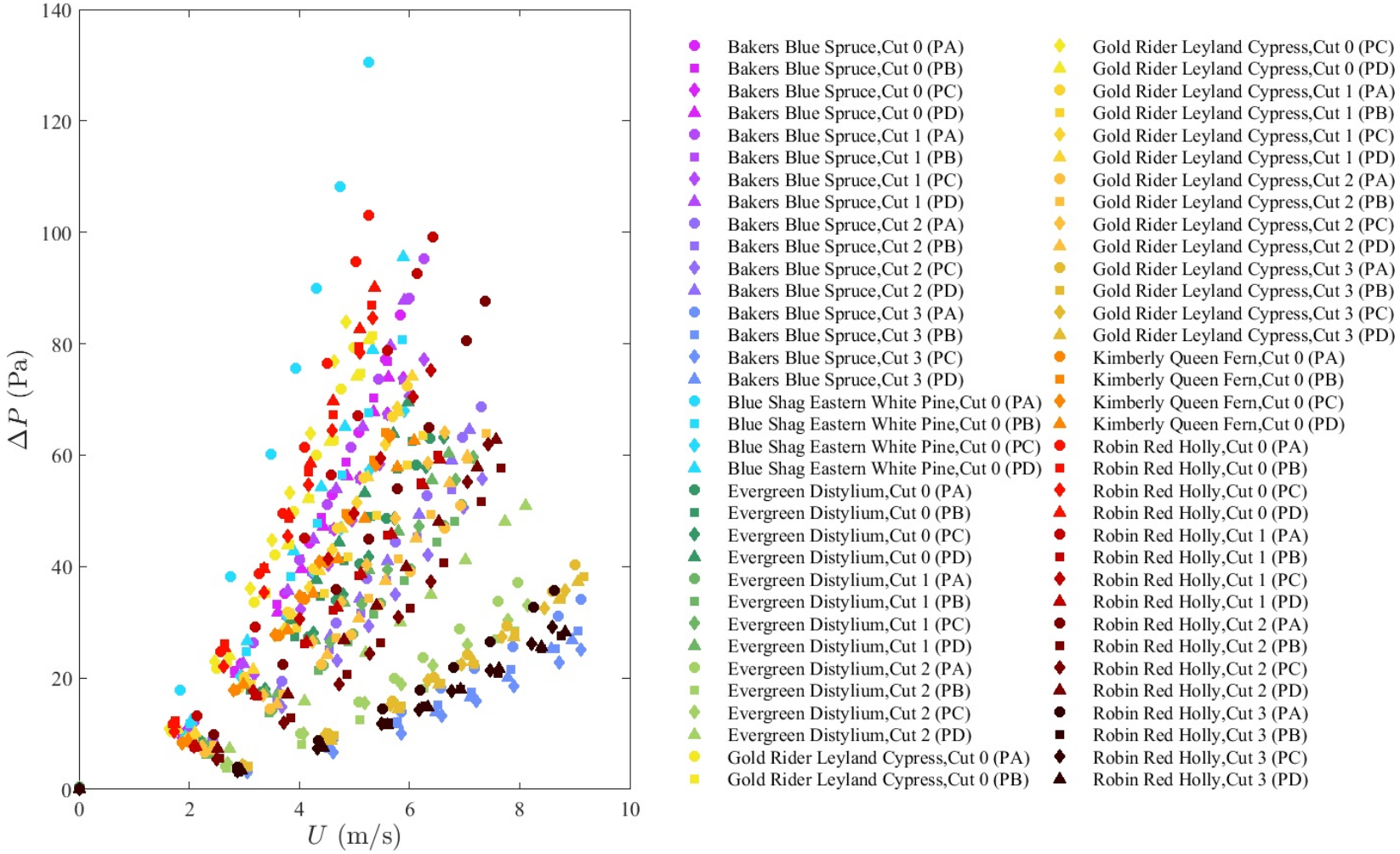

Fig. 8. Differential pressure measurements of vegetation samples subjected to a range of freestream velocities

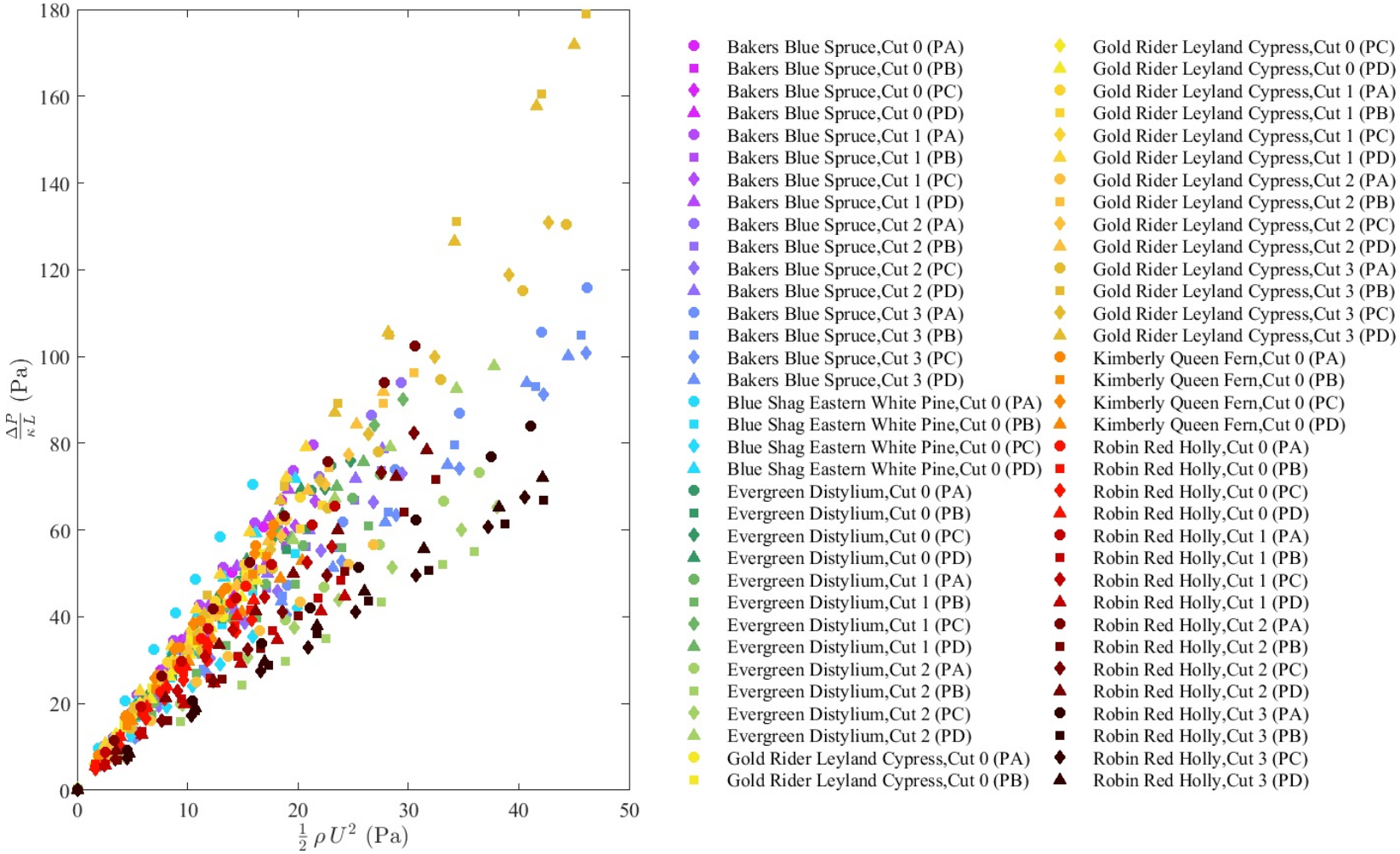

Fig. 9. Differential pressure measurements of vegetation samples over (κL) vs. dynamic pressure

Table 2. Drag Coefficient Summary of Vegetation Samples

Sample	Cut	Position	C_d	Uncertainty	Sample	Cut	Position	C_d	Uncertainty
Bakers Blue Spruce	0	A	3.6	0.4	Gold Rider Leyland Cypress	0	A	3.0	0.4
		B	3.2	0.4			B	3.3	0.4
		C	3.1	0.4			C	3.4	0.5
		D	3.0	0.4			D	3.0	0.4
	1	A	3.7	0.4		1	A	3.3	0.4
		B	3.0	0.4			B	2.9	0.3
		C	3.1	0.3			C	3.3	0.4
		D	3.6	0.4			D	3.8	0.4
	2	A	3.2	0.3		2	A	2.1	0.2
		B	2.7	0.3			B	3.2	0.3
		C	2.5	0.3			C	3.1	0.3
		D	2.8	0.3			D	3.3	0.3
	3	A	2.5	0.3		3	A	2.9	0.4
		B	2.3	0.4			B	3.8	0.5
		C	2.2	0.4			C	3.0	0.4
		D	2.3	0.4			D	3.8	0.5
Blue Shag Eastern White Pine	0	A	4.0	0.6	Kimberly Queen Fern	0	A	3.2	0.4
		B	2.5	0.3			B	2.8	0.4
		C	1.9	0.3			C	3.0	0.4
		D	3.4	0.4			D	2.4	0.3
Evergreen Distylium	0	A	3.2	0.3	Robin Red Holly	0	A	3.1	0.4
		B	2.9	0.3			B	2.6	0.3
		C	3.1	0.3			C	2.5	0.3
		D	3.4	0.4			D	2.7	0.3
	1	A	2.7	0.3		1	A	2.8	0.2
		B	2.3	0.3			B	2.0	0.2
		C	3.1	0.3			C	2.5	0.2
		D	2.9	0.3			D	1.8	0.2
	2	A	2.0	0.3		2	A	3.4	0.2
		B	1.5	0.2			B	2.2	0.2
		C	1.7	0.2			C	2.7	0.2
		D	2.6	0.3			D	2.5	0.2
						3	A	2.1	0.2
							B	1.6	0.2
							C	1.6	0.2
							D	1.7	0.2

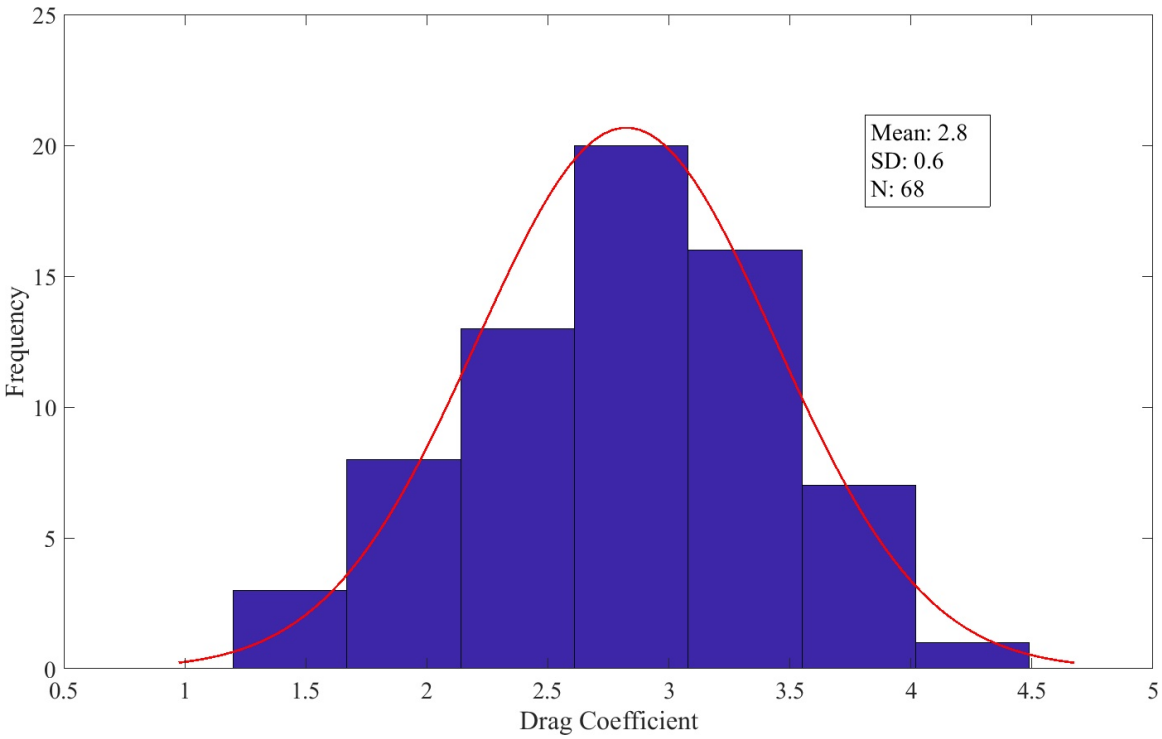

Fig. 10. Distribution of vegetation samples drag coefficients with noted mean and standard deviation values

cylinders within our wind tunnel, using both actual steel rods and empirical results from Idelchick [10]. For each of the measured vegetation samples, a comparable configuration of vertical tubes was derived such that the volume fraction, β, absorption coefficient, κ, and characteristic diameter, D, match as closely as possible (see Table 3). The characteristic diameter was calculated from Eq. 3 using the measured β and κ values and assuming a cylindrical shape factor ($C_s = \frac{1}{\pi}$). The expected pressure drop through the tube bank was either measured directly in the wind tunnel or taken from Idelchick (Eq. 6), and the corresponding drag coefficient was determined from Eq. 5.

$$\Delta P = \frac{\rho}{2} \frac{A\,Re^{-0.25}}{W^2} U^2 \tag{6}$$

In Eq. 6, A is defined as a geometric parameter determined from the tube bank configuration and Re is Reynold's number which must be greater than 3E3 for the empirical model to apply.

Figure 11 compares the drag coefficients from the Gold Rider Leyland Cypress and Bakers Blue Spruce with their tube bank equivalents. While the match is not expected to be perfect given the difference in skin fraction, shape, and so on, the drag coefficients of each configuration is comparable.

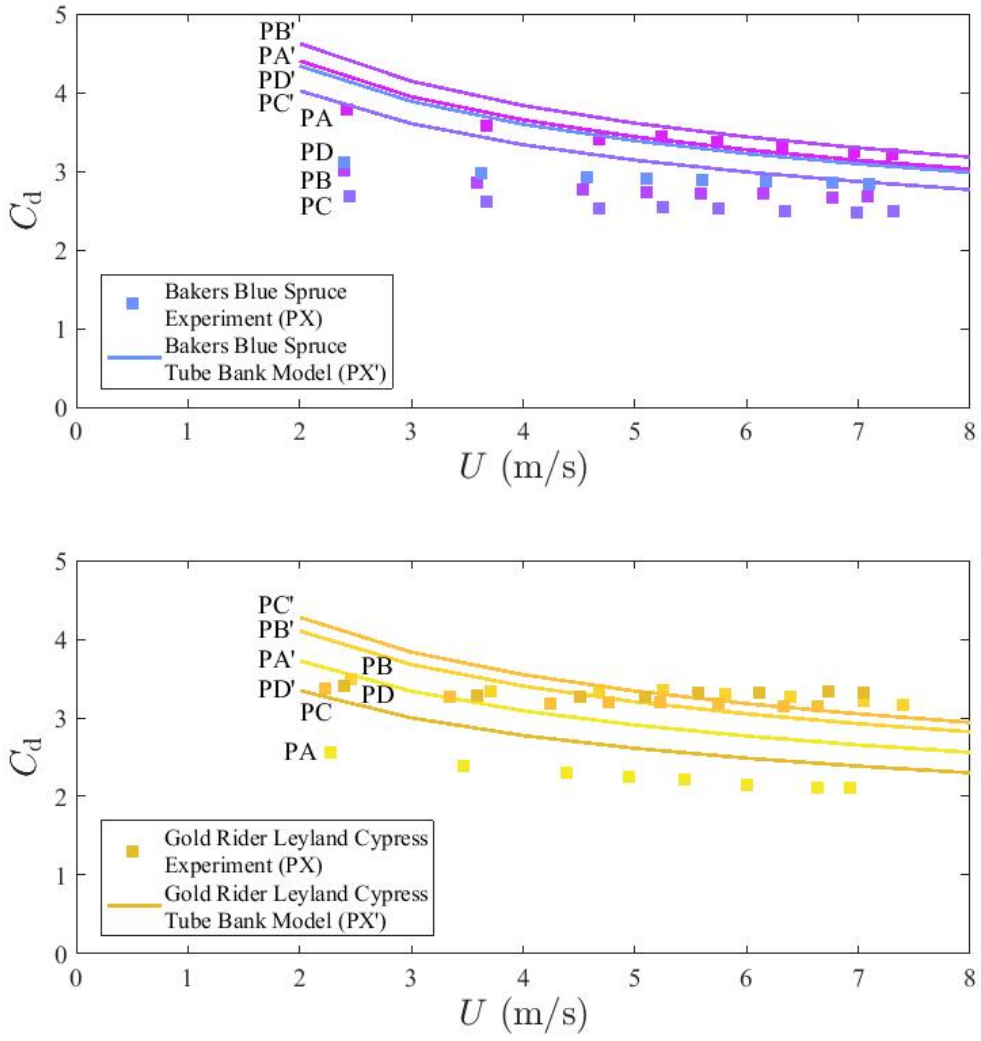

Fig. 11. Drag Coefficient comparison between vegetation sample configurations (Bakers Blue Spruce, Cut 2 and Gold Rider Leyland Cypress, Cut 2) and thier corresponding tube bank configuration with respect to velocity

Table 3. Parameters used in comparing vegetation with a comparable tube bank configuration

Pos.	β (x10^2)		κ (m^{-1})		D (mm)		Rows	Tubes/Row
	Veg.	Tubes	Veg.	Tubes	Veg.	Tubes		
Gold Rider Leyland Cypress, Cut 2								
A	1.2	1.1	1.8	1.7	8.5	9.5	4	5
B	1.2	1.2	1.3	1.3	11.6	12.6	4	3
C	1.2	1.3	1.7	1.8	9.3	10.1	5	4
D	1.2	1.2	1.3	1.3	11.9	13.8	2	5
Bakers Blue Spruce, Cut 2								
A	1.2	1.1	1.5	1.4	10.1	10.8	5	3
B	1.2	1.1	1.6	1.5	9.2	9.8	6	3
C	1.2	1.1	1.5	1.5	9.7	10.6	4	4
D	1.2	1.2	1.6	1.7	9.0	9.7	5	4

Conclusion

This report documents a series of experiments implemented to determine the absorption coefficient, pressure loss, and the solid fraction of different types of vegetation sample configurations. The primary objective of this work was to calculate the drag coefficients of "bulk" vegetation that can be incorporated into CFD models. In addition to establishing drag coefficients of "bulk" vegetation, notable findings regarding vegetation structure and similarities between drag coefficients of plant species were also discovered from this work. It cannot be concluded, however, that the findings from this work applies to all "bulk" vegetation, but exclusively to the samples studied in these experiments.

1. The calculated absorption coefficient for each sample demonstrated a strong relationship with its corresponding solid fraction.

2. The overall average drag coefficient of the bulk vegetation was found to be 2.8 with a standard deviation of 0.6. The differences between the average drag coefficients of different plant species were concluded to be non-significant suggesting that the overall average drag coefficient could be used as a constant value in CFD models of various plant types.

Acknowledgments

Matthew Bundy and Artur Chernovksy of the National Fire Research Laboratory assisted in conducting these experiments and in processing the data.

References

[1] McGrattan K, et al. (2013) *Fire Dynamics Simulator, Technical Reference Guide* National Institute of Standards and Technology, Gaithersburg, Maryland, USA, and VTT Technical Research Centre of Finland, Espoo, Finland, sixth Ed. Vol. 1: Mathematical Model; Vol. 2: Verification Guide; Vol. 3: Validation Guide; Vol. 4: Software Quality Assurance.

[2] Cao J, Tamura Y, Yoshida A (2012) Wind tunnel study on aerodynamic characteristics of shrubby specimens of three tree species. *Urban Forestry and Urban Greening* 11(4):465–476. https://doi.org/10.1016/j.ufug.2012.05.003

[3] Jalonen J, Järvelä J (2014) Estimation of drag forces caused by natural woody vegetation of different scales*. *J Hydrodynamics* 26(4):608–623. https://doi.org/10.1016/S1001-6058(14)60068-8

[4] Mayhead G (1973) Some drag coefficients for british forest trees derived from wind tunnel studies. *Agricultural Meterology* 12:123–130. https://doi.org/10.1016/0002-1571(73)90013-7

[5] Gillies JA (2002) Drag coefficient and plant form response to wind speed in three plantspecies: Burning bush (euonymus alatus), colorado blue spruce (picea pungens glauca.), and fountain grass (pennisetum setaceum). *J Geophysical Research* 107(D24):ACL 10–1–ACL 10–15. https://doi.org/10.1029/2001JD001259

[6] Ishikawa H, Amano AS, Kenta Y (2006) Flow around a living tree. *JSME International Journal Series B Fluids and Thermal Engineering* 49(4):1064–1069. https://doi.org/10.1299/jsmeb.49.1064

[7] Pimont F, Dupuy J, Linn RR, Dupont S (2009) Validation of firetec wind-flows over a canopy and a fuel-break. *Int J Wildland Fire* 18(7):775–790. https://doi.org/10.1071/WF07130

[8] Dupont S, Brunet Y (2008) Edge flow and canopy structure: a large-eddy simulation study. *Boundary Layer Meteorology* 126(1):51–71. https://doi.org/10.1007/s10546-007-9216-3

[9] Mueller E, Mell W, Simeoni A (2014) Large eddy simulation of forest canopy flow for wildland fire modeling. *Canadian J Forest Res* 44(12):1534–1544. https://doi.org/10.1139/cjfr-2014-0184

[10] Idelchick I (1994) *Handbook of Hydraulic Resistance, 3rd Edition* (CRC Press, Inc.), .